

# Enhanced alkenes epoxidation reactivity of discrete bis(8-quinolinol)oxovanadium(IV) or bis(8-quinolinol)dioxomolybdenum(VI) tethered to graphene oxide by a metal-template/metal-exchange method

Zhifang Li<sup>a</sup>, Shujie Wu<sup>a</sup>, Dafang Zheng<sup>b</sup>, Heng Liu<sup>a</sup>, Jing Hu<sup>a</sup>, Hailiang Su<sup>a</sup>, Jian Sun<sup>a</sup>, Xu Wang<sup>c</sup>, Qisheng Huo<sup>b</sup>, Jingqi Guan<sup>a,\*</sup>, Qiubin Kan<sup>a,\*</sup>

<sup>a</sup> College of Chemistry, Jilin University, Changchun, 130023, PR China

<sup>b</sup> State Key Laboratory of Inorganic Synthesis and Preparative Chemistry, College of Chemistry, Jilin University, Changchun, 130012, PR China

<sup>c</sup> State Key Laboratory of Supramolecular Structure and Materials, Jilin University, Changchun, 130012, PR China



## ARTICLE INFO

### Article history:

Received 30 June 2013

Received in revised form

27 September 2013

Accepted 21 October 2013

Available online 29 October 2013

### Keywords:

Grapheme oxide

Epoxidation

Styrene

Metal-template method

8-Quinolinol complexes

## ABSTRACT

A series of imprinted catalysts were obtained by covalent attachment of discrete bis(8-quinolinol)oxovanadium(IV) or bis(8-quinolinol)dioxomolybdenum(VI) complex onto graphene oxide (GO) through the metal-template/metal-exchange method to control the distribution of covalently attached independent ligands, which were examined as catalysts in the epoxidation of alkenes using *t*-butylhydroperoxide (TBHP) or H<sub>2</sub>O<sub>2</sub> as oxidant in comparison with their homogeneous counterparts and materials synthesized by random grafting of the ligand. The prepared catalysts were characterized by XRD, N<sub>2</sub> adsorption/desorption, TEM, FT-IR, diffusion reflection UV-visible, ICP-AES, TG, Raman, EPR, N element analysis and XPS. FT-IR, diffusion reflection UV-visible, ICP-AES, TG, N element analysis, Raman and XPS results showed that oxovanadium(IV) or dioxomolybdenum(VI) complexes were successfully grafted on GO. XRD, N<sub>2</sub> adsorption/desorption and TEM results indicated that the structures of the samples were well preserved. EPR results revealed that the materials synthesized by the metal-template method had better site-isolation compared with conventional materials. Furthermore, these imprinted oxovanadium(IV) or dioxomolybdenum(VI) complex catalysts are efficient and recyclable, which exhibit higher activity and higher selectivity to target product than either their homogeneous ones or randomly grafted analogues due to better site-isolation.

© 2013 Elsevier B.V. All rights reserved.

## 1. Introduction

The catalytic epoxidation of alkenes plays a major role in synthesis of the corresponding epoxides, which is widely used in the production of fine chemicals and chemical intermediates [1–4]. Transition metal complexes containing redox active transition metals (Fe, V and Mo) have been reported as important homogeneous catalysts for alkenes oxidation [5–7]. However, most of the homogeneous catalysts suffer from drawbacks such as deactivation, difficult recovery and recycling of the catalysts. To overcome these drawbacks, heterogeneous catalysts prepared by immobilizing the homogeneous complexes onto insoluble solid supports have been developed [8,9]. Since the reactivity of many tethered catalysts is less than the corresponding homogeneous counterparts for

olefin oxidation, new method for preparing heterogeneous epoxidation catalysts is encouraged.

For the heterogenization of discrete homogeneous catalysts, recent advances principally adopt immobilization of single, multidentate ligands such as porphyrin, salen, or 1,4,7-triazacyclononane onto supports in order to provide metal coordination for catalytic activity [10,11]. Random grafting of such complexes onto a support makes certain that the homogeneous coordination sphere and catalytic reactivity are retained. Furthermore, reports of covalent imprinting of coordination sites composed of several independent ligands, such as bis(8-quinolinol)oxovanadium(IV) and bis(8-quinolinol)dioxomolybdenum(VI) are very few. The desirable covalent imprinted coordination sites for a single metal created from several independent ligands (e.g. 1,10-phenanthroline) was achieved by Stack etc. [12,13]. The imprinted catalysts possess better site isolation in consideration of the homogeneity of grafted metal complexes and show better consistency in the epoxidation

\* Corresponding authors. Tel.: +86 431 88499140, fax: +86 431 88499140.

E-mail addresses: [guanjq@jlu.edu.cn](mailto:guanjq@jlu.edu.cn) (J. Guan), [qkan@mail.jlu.edu.cn](mailto:qkan@mail.jlu.edu.cn) (Q. Kan).

reaction than the corresponding homogeneous catalysts and randomly grafted catalysts. Site-isolated bis(1,10-phenanthroline) complexes on SBA-15 mesoporous silica were prepared via a metal-template/metal-exchange method. Using this strategy, the catalysts with the templated ferrous and Mn<sup>II</sup> bisphen sites showed higher activity and selectivity than the analogous homogeneous catalyst or immobilized Fe and Mn catalysts prepared by random grafting of the ligand on SBA-15.

Compared with mesoporous silicates such as MCM-41 and SBA-15, graphene oxide (GO) has unique nanostructure (monolayer), ample oxygen carrying functionalities on its basal planes and at its edges (hydroxyl, epoxide, and carboxylic groups), excellent mechanical strength and hydrothermal stability, and the prospect of various applications such as composite materials, catalysis, optoelectronics, supercapacitors, memory devices and as a drug delivery agent [14–21]. It is already well known that GO can be synthesized by the exfoliation of graphitic oxide. For the first time graphite oxide was synthesized by the oxidation of graphite by William et al. in 1958 [22]. Monomolecular sheets GO could be obtained by the exfoliation of this graphitic oxide in organic solvent [23]. Recently, Mungse et al. [14] reported that the prepared graphene-bound oxo-vanadium Schiff base catalyst was highly efficient and showed comparable catalytic reactivity for the oxidation of various alcohols, diols, and α-hydroxyketones to carbonyl compounds using TBHP as an oxidant. Furthermore, as far as we are aware, the covalent attachment of a discrete bis(8-quinolinol) oxovanadium(IV) and dioxomolybdenum(VI) complexes onto GO by the metal-template/metal-exchange method has not been reported.

Previously, we found that tethering of transition metals oxovanadium(IV) and dioxomolybdenum(VI) complexes onto SBA-15 material are highly active in the epoxidation of cyclooctene or styrene [24,25]. However, metal complexes heterogenized by random grafting are not very stable during the process of reaction and the metal species would be partly leached into the solution in the experimental process. Herein we first report design and characterization of the covalent attachment of discrete bis(8-quinolinol) oxovanadium(IV) and dioxomolybdenum(VI) complexes onto GO by the metal-template/metal-exchange method. For comparison, their homogeneous counterparts and the randomly ligand-grafted heterogeneous analogues were additionally prepared. Furthermore, their catalytic properties in the epoxidation of alkenes (cyclooctene, styrene, geraniol or 1-octene) using TBHP or H<sub>2</sub>O<sub>2</sub> as oxidant were investigated.

## 2. Experimental

### 2.1. Materials

Graphite powder, H<sub>2</sub>SO<sub>4</sub>, KMnO<sub>4</sub>, 30% H<sub>2</sub>O<sub>2</sub>, V<sub>2</sub>O<sub>5</sub>, VOSO<sub>4</sub>, 8-hydroxyquinoline, hydrochloric acid, acetylacetone, ZnCl<sub>2</sub>, HCHO (W=38%), Zn(OAc)<sub>2</sub>·2H<sub>2</sub>O, 3-mercaptopropyltrimethoxysilane (3-MPTMS), MoO<sub>3</sub>, DMF and all organic solvents are A.R. grade. Na/diphenylketone ketyl was used to dry tetrahydrofuran (THF), and then THF is distilled under N<sub>2</sub> atmosphere, and is stored over 4A molecular sieves.

### 2.2. Synthetic procedures (Scheme 1)

The procedure for the covalent attachment of 8-quinolinol complexes of oxovanadium(IV) and molybdenum dioxide(VI) to GO (graphene oxide) by random grafting and metal-template/metal-exchange method to form VO<sup>IV</sup>T, VO<sup>IV</sup>G, MoO<sub>2</sub><sup>VI</sup>T and MoO<sub>2</sub><sup>VI</sup>G, respectively, is depicted in Scheme 1 and described as follows.

### 2.2.1. Synthesis of GO

GO was prepared according to the literatures [14,22,26–28]. Typically, graphite powder and concentrated H<sub>2</sub>SO<sub>4</sub> was added to a 250 ml three-necked flask. The mixture was stirred in an ice bath for 120 min. 6.0 g KMnO<sub>4</sub> was then added into the mixture gradually under vigorous stirring and the reaction mixture was stirred at room temperature for 2 h. After that, the mixture was stirred at 35 °C for 30 min and 92 ml deionized water was added under vigorous stirring. Soon afterwards, the mixture was heated to 95 °C for 15 min. At last, the mixture was transferred to a 1000 ml beaker and 280 ml deionized water and 5 ml 30% H<sub>2</sub>O<sub>2</sub> solution was added. The required brown product was obtained by filtering, washing with a large amount of 5% HCl solution and deionized water and then drying.

### 2.2.2. Synthesis of bis(5-chloromethyl-8-quinolinol)zinc(II) ( $[Zn^{II}(1^C)_2]H_2O$ )

5-Chloromethyl-8-quinolinol was prepared and characterized as described in our early work [29]. In a typical procedure, 11.68 g 8-hydroxyquinoline (8-Q), 12.8 ml HCHO and 1.2 g ZnCl<sub>2</sub> were added to a 250 ml three-necked flask. 100 ml concentrated HCl was then added into the mixture gradually under vigorous stirring. The reaction mixture was stirred at room temperature for 24 h. After finishing the reaction and keeping reaction product standing, the required yellow product was obtained by filtering, washing with acetone and drying. The dried sample was denoted as 1<sup>C</sup>-HCl.

Bis(5-chloromethyl-8-quinolinol)zinc(II) was also prepared and characterized as described in our early work [29]. As a typical run, 2.5 mmol 1<sup>C</sup>-HCl and 0.275 g Zn(OAc)<sub>2</sub>·2H<sub>2</sub>O were dried in advance at 100 °C for 1 h. 1<sup>C</sup>-HCl was dispersed in a 50 ml two-necked flask containing 25 ml dried THF. Under stirring, 0.35 ml Et<sub>3</sub>N was then added into the mixture. The reaction mixture was stirred at room temperature for 1 h. After that, 0.275 g Zn(OAc)<sub>2</sub>·2H<sub>2</sub>O was added to the stirred solution. The mixture was stirred under N<sub>2</sub> atmosphere for 24 h. The required green solid was obtained by filtering, washing with tetrahydrofuran and drying. The obtained product was denoted as  $[Zn^{II}(1^C)_2]H_2O$ .

### 2.2.3. Synthesis of VO(IV) acetylacetonate

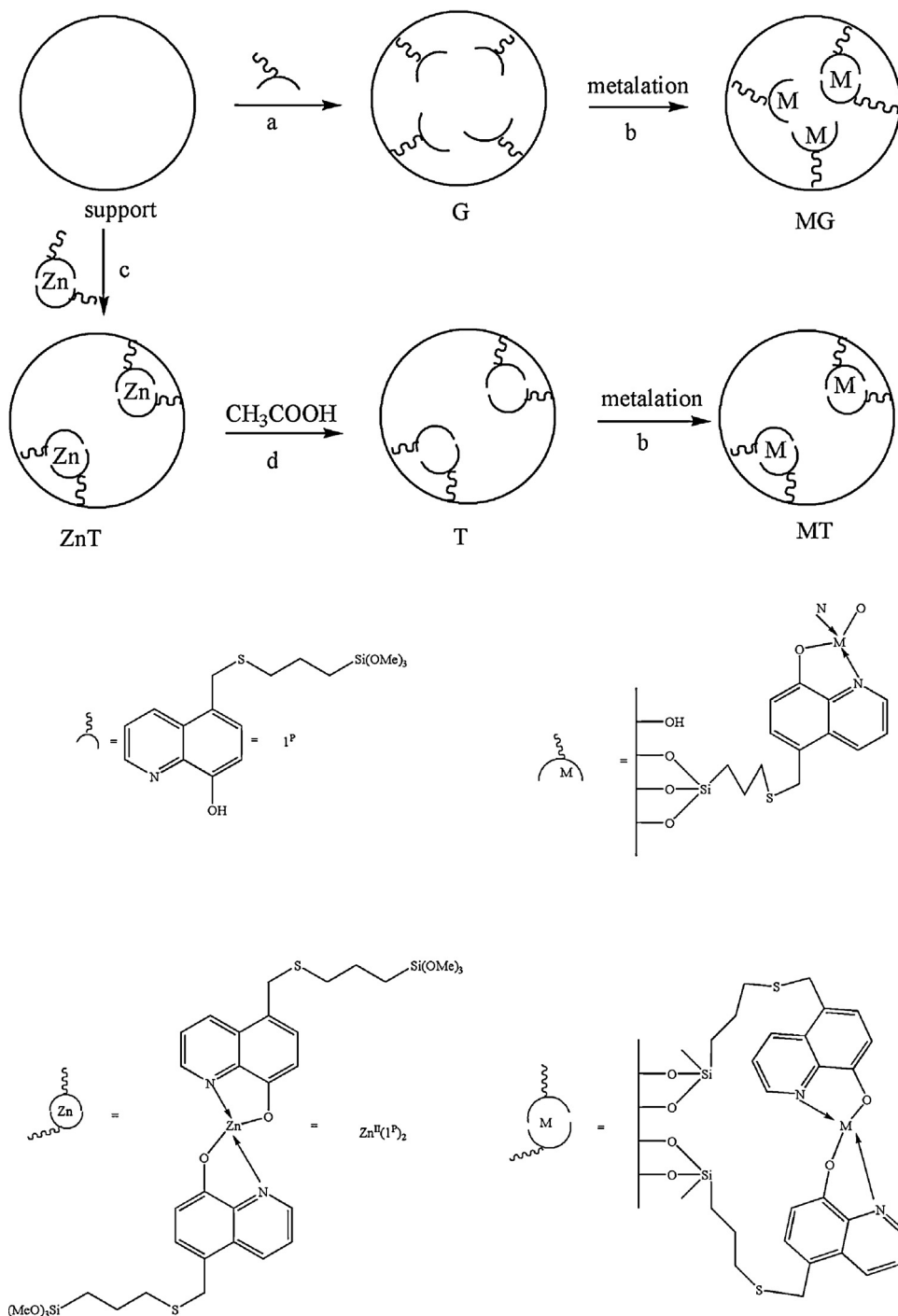
VO(IV) acetylacetonate was prepared and characterized as described in our early work [29]. In a typical procedure, 2.5 g V<sub>2</sub>O<sub>5</sub> and 50 ml acetylacetone were added to flask. The mixture was refluxed at 80 °C for 24 h. The solid was then filtered, washed abundantly with acetone, and dried. The turquoise solid was denoted as VO(acac)<sub>2</sub>.

### 2.2.4. Synthesis of MoO<sub>2</sub>Cl<sub>2</sub>(dmf)<sub>2</sub>

MoO<sub>2</sub>Cl<sub>2</sub>(dmf)<sub>2</sub> was prepared and characterized as described in our early work [30]. In a typical synthesis, the mixture of 1.0 g MoO<sub>3</sub> and 10 ml (6 M) HCl was heated to boil until most of MoO<sub>3</sub> was dissolved, then the mixture was quickly cooled down to room temperature. After that, the clear solution was obtained by filtered. 2.5 ml DMF was added to the clear solution and the mixture was stirred for 2 h. The white solid was obtained by filtered, washed with acetone, and dried.

### 2.2.5. Synthesis of VO<sup>IV</sup>T and MoO<sub>2</sub><sup>VI</sup>T by metal-template/metal-exchange method

Zn<sup>II</sup>T was prepared according to our previous work with slight modification [29]. For Zn<sup>II</sup>T preparation, 0.5 mmol pre-dried  $[Zn^{II}(1^C)_2]H_2O$  and 0.18 ml 3-MPTMS were added to a 25 ml two-necked flask containing 20 ml dry THF under N<sub>2</sub> atmosphere. Afterwards, the mixture was refluxed at 65 °C for 15 h. Finally, 10 ml dry THF were added and then 0.625 g GO was dispersed by ultrasound.



**Scheme 1.** Schematic outlines of the covalent attachment of 1<sup>P</sup> to the GO via random grafting and metal-templating method to form MG and MT [M = VO(IV) and MoO<sub>2</sub>(VI)], respectively: (a) random grafting of 1<sup>P</sup>; (b) metalation; (c) formation of Zn<sup>II</sup>T followed by covalent attachment; (d) demetalation with CH<sub>3</sub>COOH.

The mixture was refluxed for 1 d under N<sub>2</sub> atmosphere. The sample was filtered, washed repeatedly with a large amount of THF and dried. Template T was prepared by refluxing 0.5 g of Zn<sup>II</sup>T with 10 ml acetic acid at 80 °C for 1 d and then filtering and washing with plentiful water. This process can be repeated twice.

VO<sup>IV</sup>T was prepared by adding of a certain amount of VO(acac)<sub>2</sub> into the methanol solution containing 0.5 g T, stirring at room temperature for 24 h, filtering, washing with CH<sub>2</sub>Cl<sub>2</sub> and extracting with CH<sub>2</sub>Cl<sub>2</sub>.

For MoO<sub>2</sub><sup>VI</sup>T preparation, 0.051 g Na<sub>2</sub>CO<sub>3</sub>, 20 ml CHCl<sub>3</sub>, 0.158 g MoO<sub>2</sub>Cl<sub>2</sub>(dmf)<sub>2</sub> and 0.6 g T were added to a beaker. The mixture was

stirred for 24 h. The sample was filtered and washed with abundant water and extracted with CH<sub>2</sub>Cl<sub>2</sub>.

#### 2.2.6. Synthesis of VO<sup>IV</sup>G and MoO<sub>2</sub><sup>VI</sup>G by random grafting method

G was prepared through the reaction of 5-chloromethyl-8-quinolinol (1<sup>C</sup>-HCl), 3-MPTMS and GO. Typically, 1.6 mmol 1<sup>C</sup>-HCl, 1.6 mmol triethylamine and 0.29 ml 3-MPTMS were added into a 25 ml two-necked flask containing 20 ml dry THF under N<sub>2</sub> atmosphere. The mixture was refluxed at 65 °C for 15 h. Subsequently, 10 ml dry THF was added and then 1.0 g GO was dispersed by

ultrasound. After vigorous stirring for 24 h, the solid was then filtered, washed with  $\text{CH}_2\text{Cl}_2$  and dried.

For  $\text{VO}^{\text{IV}}\text{G}$  preparation, 0.5 g G and 0.25 mmol  $\text{VO}(\text{acac})_2$  were added into the methanol solution. The mixture was stirred at room temperature for 24 h. The sample was filtered and washed with methanol and extracted with  $\text{CH}_2\text{Cl}_2$ .

$\text{MoO}_2^{\text{VI}}\text{G}$  was prepared by addition of 0.051 g  $\text{Na}_2\text{CO}_3$  and 0.158 g  $\text{MoO}_2\text{Cl}_2(\text{dmf})_2$  into the  $\text{CHCl}_3$  solution containing 0.6 g T. The mixture was stirred at room temperature for 24 h, filtered, washed with  $\text{CHCl}_3$  and extracted with  $\text{CH}_2\text{Cl}_2$ .

#### 2.2.7. Synthesis of the neat complexes $\text{VO}^{\text{IV}}\text{N}$ and $\text{MoO}_2^{\text{VI}}\text{N}$

$\text{VO}^{\text{IV}}\text{N}$  was prepared and characterized as described in our early work [29]. 1.25 mmol  $\text{VO}(\text{acac})_2$  was added into the methanol solution containing 2.5 mmol 8-quinolinol. The mixture was stirred at room temperature for 24 h. The sample was filtered and washed with large quantities of methanol.

$\text{MoO}_2^{\text{VI}}\text{N}$  was prepared by addition of 0.05 mmol  $\text{MoO}_2\text{Cl}_2(\text{dmf})_2$  into the  $\text{CHCl}_3$  solution containing 0.1 mmol 8-quinolinol. The mixture was stirred at room temperature for 24 h, filtered, and washed with large quantities of  $\text{CHCl}_3$ . FT-IR (KBr pellets,  $\text{cm}^{-1}$ ): 1627 (C=C), 1570, 1491 (py), 898 (Mo=O), 527 (Mo-O), 469 (Mo-N).

### 2.3. Characterization

The infrared spectra were recorded in KBr disks using a NICOLET impact 410 spectrometer. Powder X-ray diffractometry (XRD) measurements were performed on a Shimadzu XRD-6000 diffractometer using a Ni-filtered  $\text{Cu K}\alpha$  radiation scanning from  $5^\circ$  to  $40^\circ$  ( $2\theta$ ). Samples were dried previously and pulverized.  $\text{N}_2$  adsorption-desorption isotherms were measured with a Micromeritics ASAP 2020 system at liquid  $\text{N}_2$  temperature. Before measurements, the sample was outgassed at  $130^\circ\text{C}$  for 6 h. The BET surface area was calculated using the Brunauer–Emmett–Teller (BET) method. Diffuse reflectance UV-vis spectra were recorded from 200 to 800 nm on a Shimadzu UV-3600 spectrophotometer using  $\text{BaSO}_4$  as a reference. Metal content was estimated by inductively coupled plasma atomic emission spectroscopy (ICP-AES) analysis conducted on a Perkin-Elmer emission spectrometer. Elemental analyses of nitrogen were obtained with a VarioEL CHN elemental analyzer. X-ray photoelectron spectroscopy (XPS) was carried out on an ESCALAB 250 X-ray electron spectrometer using  $\text{AlK}\alpha$  radiation. EPR spectra were recorded at room temperature on a JES-FA 200 spectrometer. Morphological features of the materials were characterized by a JEOL JEM-2010 transmission electron microscope at an accelerating voltage of 200 kV. Raman spectra were recorded on a Renishaw Raman system model 1000 spectrometer with an excitation wavelength of 514 nm. TG analyses were performed on a Shimadzu DTA-60 working with the heating rate of  $10^\circ\text{C min}^{-1}$  from  $25^\circ\text{C}$  to  $600^\circ\text{C}$  under flowing  $\text{N}_2$ .

### 2.4. Catalytic tests

The catalytic epoxidation of cyclooctene, styrene, geraniol or 1-octene was carried out in a 5 ml flask equipped with a reflux condenser. Typically, substrate (1 mmol), solvent ( $\text{MeCN}$  or  $\text{CHCl}_3$ , 1 ml), dodecane (0.5 mmol, internal standard) and catalyst (10 mg) were mixed. The mixture was heated to  $70^\circ\text{C}$ , and then oxidant (TBHP or  $\text{H}_2\text{O}_2$ , 5 mmol) was introduced. The reaction products were analyzed by gas chromatography (GC) with a Shimadzu GC-8A (Japan) instrument equipped using an HJ-5 capillary column and FID detector. At the end of the reaction, the catalyst was filtered off, washed with copious solvent, and dried. The catalyst was then reused in the next reaction without further purification.

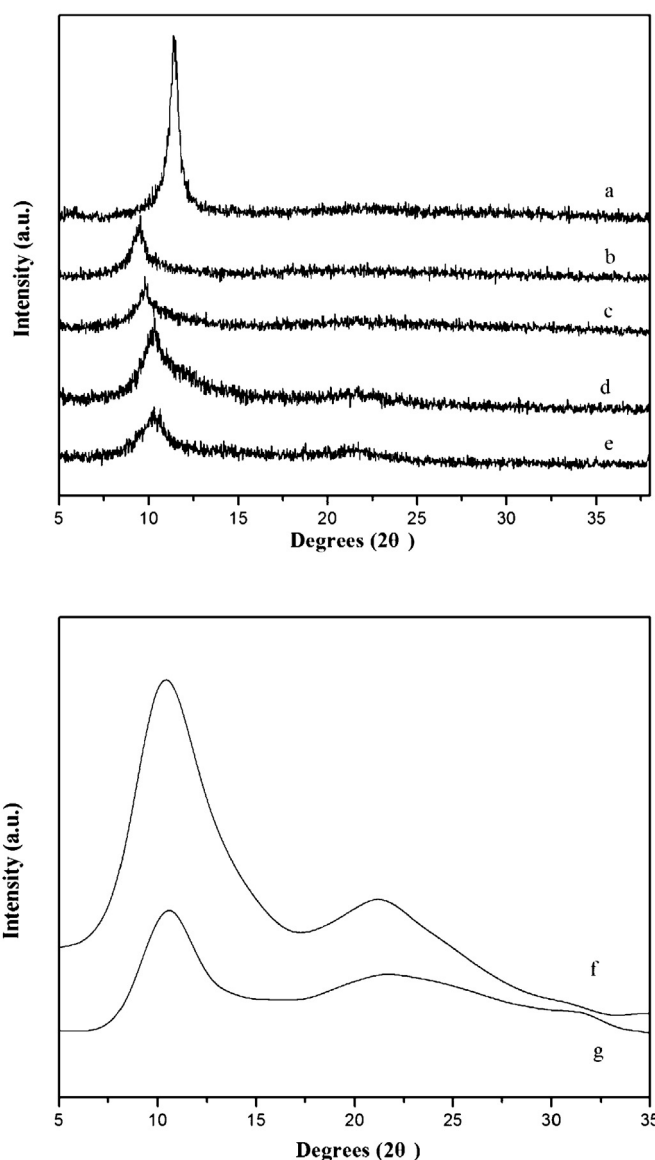
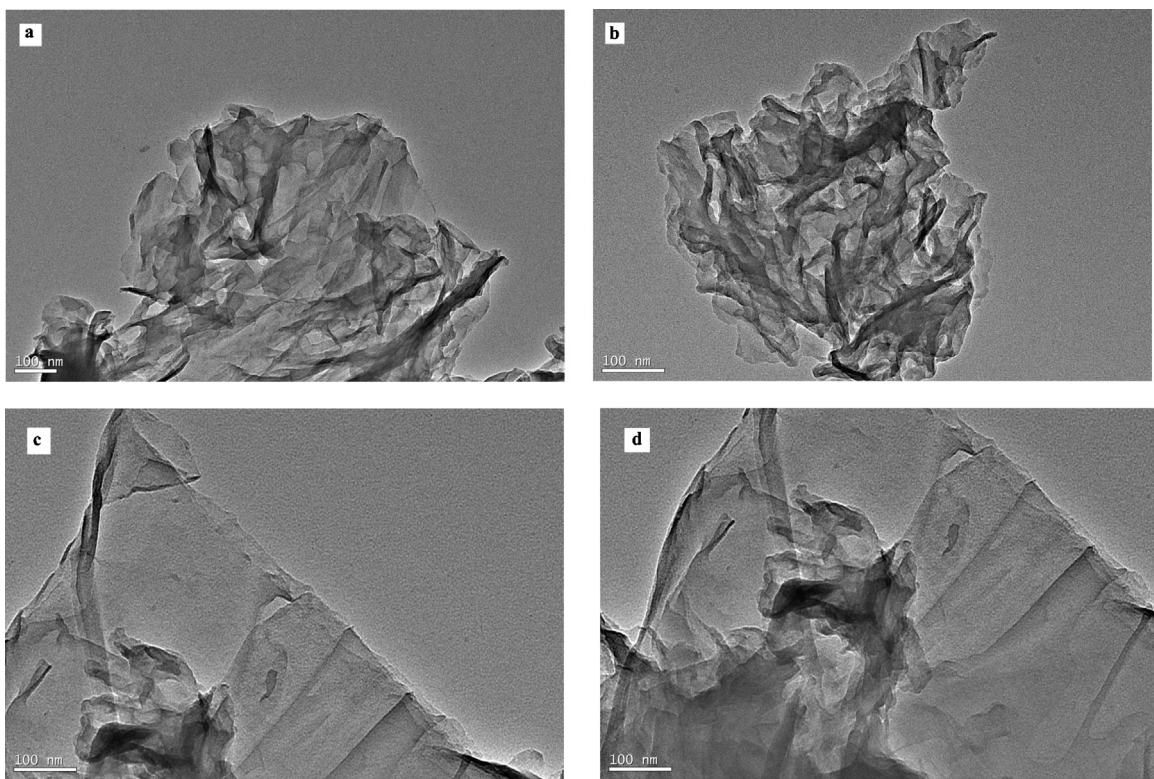


Fig. 1. High angle X-ray diffraction patterns of (a) GO, (b)  $\text{Zn}^{\text{II}}\text{T}$ , (c) T, (d)  $\text{VO}^{\text{IV}}\text{T}$ , (e)  $\text{VO}^{\text{IV}}\text{G}$ , (f)  $\text{MoO}_2^{\text{VI}}\text{T}$  and (g)  $\text{MoO}_2^{\text{VI}}\text{G}$ .

## 3. Results and discussion

### 3.1. Structural characteristics of catalysts

The powder XRD patterns of pure support GO and the covalent attachments of 8-quinolinol complex catalysts are shown in Fig. 1. For GO (Fig. 1a), the peak at around  $11.5^\circ$  can be assigned to the (001) reflection of graphite oxide [14,31,32]. It is clear that oxygen species were successfully inserted into the graphitic layers [33,34]. For  $\text{Zn}^{\text{II}}\text{T}$ , the intensity of the (001) reflection of graphene oxide are significantly reduced, which might be due to the 8-quinolinol complexes distribution in the GO. Moreover, the diffraction peak at ca.  $2\theta = 11.5^\circ$  does not disappear, which clearly indicates that the structure of graphene oxide was not destroyed during the process of refluxing of T. A similar pattern is found for all covalent attachment of 8-quinolinol complexes catalysts (Fig. 1d and e), suggesting that they are similar in graphene oxide layer. However, the very weak and broad diffraction peak centered at  $21.2^\circ$  is seen for  $\text{MoO}_2^{\text{VI}}\text{T}$  and  $\text{MoO}_2^{\text{VI}}\text{G}$  (Fig. 1f and g), indicating that part of the developed catalysts is closer to graphene [14].



**Fig. 2.** TEM images of (a) VO<sup>IV</sup>T, (b) VO<sup>IV</sup>G, (c) MoO<sub>2</sub><sup>VI</sup>T and (d) MoO<sub>2</sub><sup>VI</sup>G.

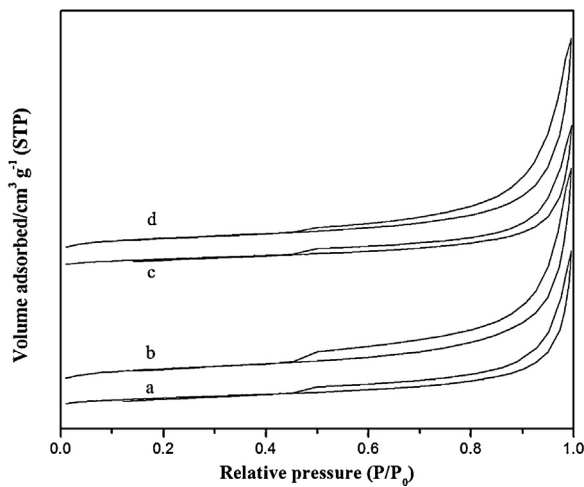


**Fig. 3.** N<sub>2</sub> adsorption/desorption isotherms profiles of (a) VO<sup>IV</sup>T, (b) VO<sup>IV</sup>G, (c) MoO<sub>2</sub><sup>VI</sup>T and (d) MoO<sub>2</sub><sup>VI</sup>G.

**Fig. 2** shows the transmission electron microscopy (TEM) images of the templated catalysts and randomly ligand-grafted heterogeneous catalysts. It is obvious that all the samples have layers structure (monolayers or just a few layers) and the crumpled nanosheets are in an aggregated phase. The N<sub>2</sub> adsorption/desorption isotherms of the templated catalysts and randomly ligand-grafted heterogeneous catalysts are depicted in **Fig. 3**. The supported materials maintain the characteristics of type IV isotherms. The BET surface area is 27, 36, 26 and 33 m<sup>2</sup>/g for VO<sup>IV</sup>T, VO<sup>IV</sup>G, MoO<sub>2</sub><sup>VI</sup>T and MoO<sub>2</sub><sup>VI</sup>G, respectively.

### 3.2. Spectroscopic characterization

**Fig. 4** shows the FT-IR spectra of the pure support and supported complexes. The spectra of the pure support GO exhibited characteristic bands at 3386, 1728, 1620, 1368, 1220 and 1054 cm<sup>-1</sup> (**Fig. 4a**), associated with the stretching mode of O-H, C=O, C=C, =C-H, C-O and C-O-C, respectively [14,26]. Moreover, the spectra of Zn<sup>II</sup>T (**Fig. 4b**) shows peaks in the region of 1600–1300 cm<sup>-1</sup> due to the C-O, C-N and aromatic ring vibrations of 8-quinolinol, verifying that Zn<sup>II</sup>T has been successfully prepared. The characteristic bands of T (**Fig. 4c**) still have in common with the Zn<sup>II</sup>T in the region of 1600–1300 cm<sup>-1</sup>, indicating that the structure of 8-quinolinol was not destroyed after removing Zn. The characteristic bands of 8-quinolinol can also be found in VO<sup>IV</sup>T and VO<sup>IV</sup>G (**Fig. 4d** and e). Similar results were obtained for MoO<sub>2</sub><sup>VI</sup>T and MoO<sub>2</sub><sup>VI</sup>G (**Fig. 4g** and h).

**Fig. 5** exhibits UV-vis spectra of homogeneous analogues, the pure support and as-prepared tethered 8-quinolinol on GO nanosheets catalysts. Compared with homogeneous analogues and the pure support, the absorption bands in the range of 200–400 nm are observed in all of the tethered catalysts, which are assigned to n-π\*, π-π\* ligand charge transfer [35], suggesting that the 8-quinolinol ligand has been anchored onto GO. The d-d transitions at ca. 550 nm are observed for VO<sup>IV</sup>T and VO<sup>IV</sup>G, indicating that oxovanadium(IV) complexes have been incorporated onto the surface of GO. Nonetheless, there is no d-d transition for the supported molybdenum catalysts, which is in accordance with our early work [24].

Raman spectroscopy was employed to determine ordered and disordered crystal structures of carbon materials, such as graphite, graphene and GO and so on. G band is generally attributed to the E<sub>2g</sub> phonon of C sp<sup>2</sup> atoms and D band is a breathing mode of κ-point phonons of A<sub>1g</sub> symmetry [36,37]. Raman spectra were carried out for all of the catalysts as shown in **Fig. 6**. The spectra of all of the

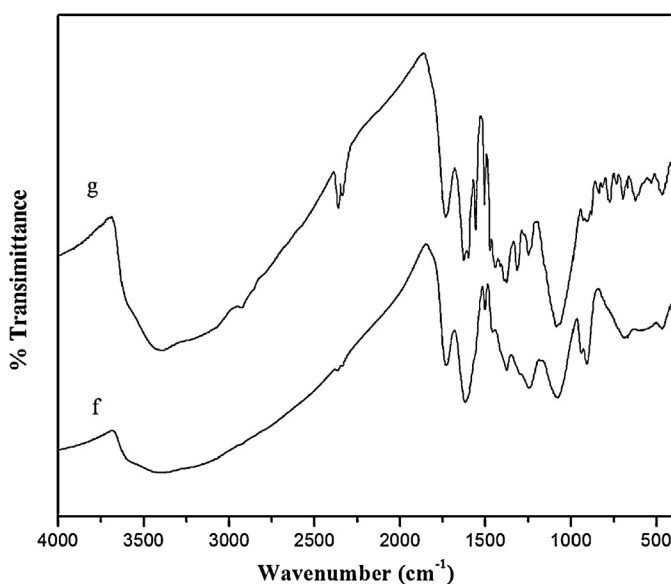
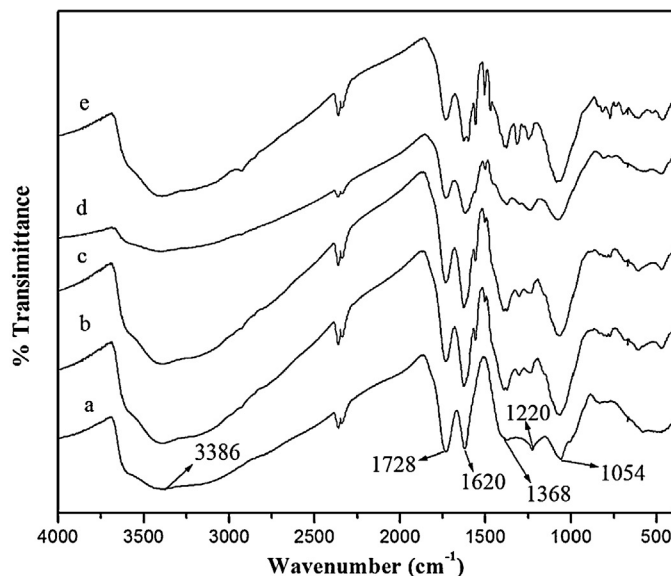


**Fig. 4.** FT-IR spectra of (a) GO, (b) Zn<sup>II</sup>T, (c) T, (d) VO<sup>IV</sup>T, (e) VO<sup>IV</sup>G, (f) MoO<sub>2</sub><sup>VI</sup>T and (g) MoO<sub>2</sub><sup>VI</sup>G.

samples show two strong bands at ca. 1350 and 1588 cm<sup>-1</sup> due to the well-defined D band and G band, respectively.  $I_D/I_G$  (the Raman intensity ratio of D and G bands) has been regarded as a unique characteristic tool to investigate the degree of graphitization in graphitic materials [38]. The values of  $I_D/I_G$  are depicted in Fig. 1S for all of the catalysts. The values of  $I_D/I_G$  in supported catalysts decreased notably compared to that in the GO (Fig. 1S), indicating that the size of the in-plane sp<sup>2</sup> domains increases and the covalent attachment of 8-quinolinol complexes to GO via random grafting by metal-template method exhibits a comparatively low degree of defects [39,40].

### 3.3. TG and EPR studies

TG profiles of the pure support GO, VO<sup>IV</sup>T, VO<sup>IV</sup>G, MoO<sub>2</sub><sup>VI</sup>T and MoO<sub>2</sub><sup>VI</sup>G are presented in Fig. 7. The TG curve of graphene oxide shows two regions of weight loss (Fig. 7a). The first minor weight loss below 180 °C is due to the loss of the physically adsorbed

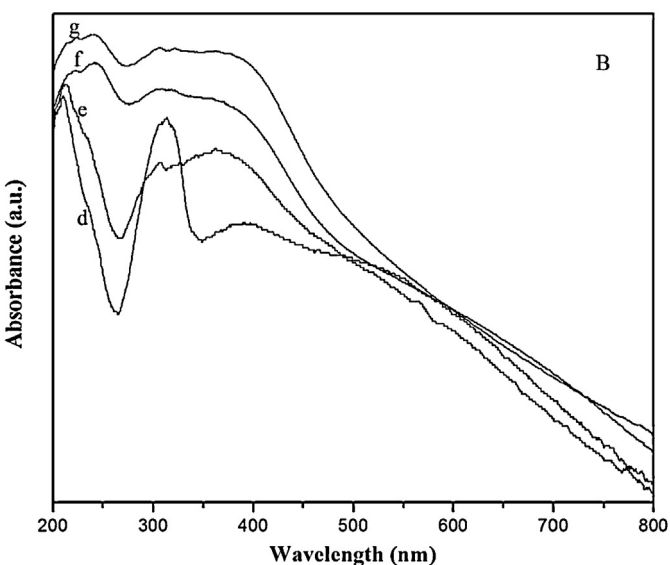
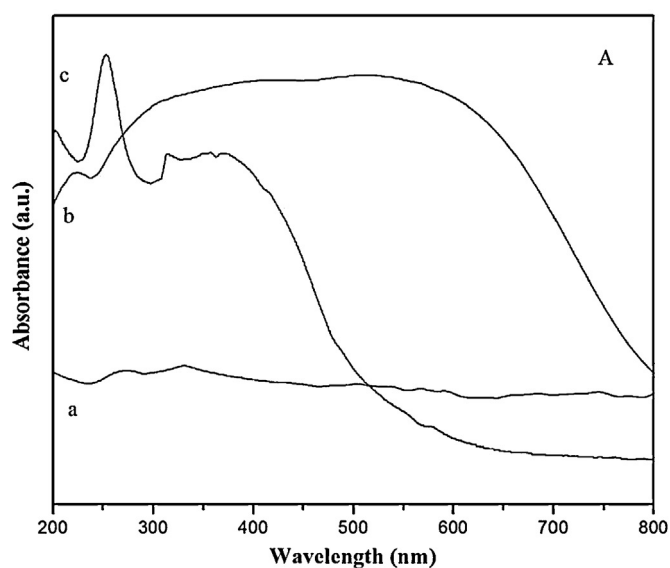


**Fig. 5.** UV-visible spectra of (A), (a) GO, (b)VO<sup>IV</sup>N, (c)MoO<sub>2</sub><sup>VI</sup>N, (B), (d) VO<sup>IV</sup>T, (e) VO<sup>IV</sup>G, (f) MoO<sub>2</sub><sup>VI</sup>T and (g) MoO<sub>2</sub><sup>VI</sup>G.

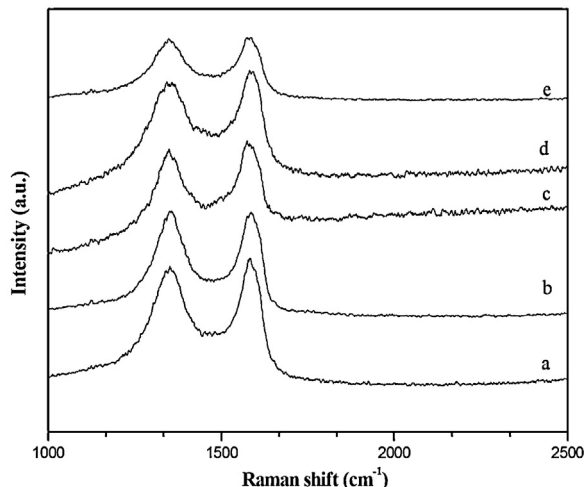


**Fig. 6.** Raman spectra (G and D bands) of (a) GO, (b) VO<sup>IV</sup>T and (c) VO<sup>IV</sup>G, (d) MoO<sub>2</sub><sup>VI</sup>T and (e) MoO<sub>2</sub><sup>VI</sup>G.

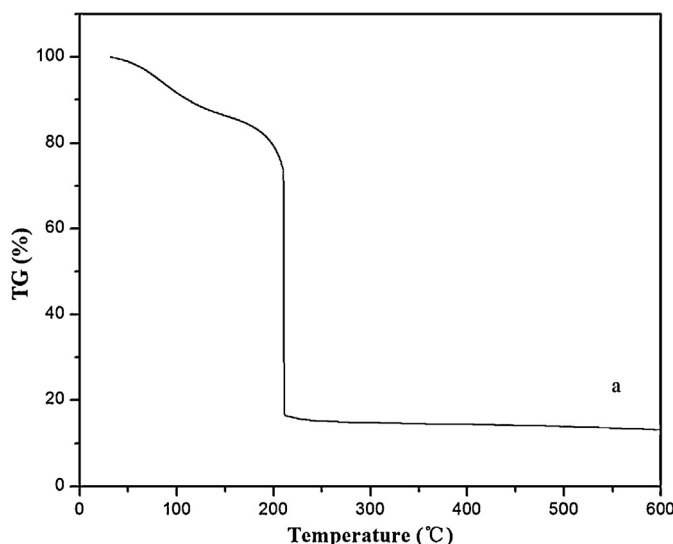


Fig. 7. TG curves of (a) GO, (b) VO<sup>IV</sup>T, (c) VO<sup>IV</sup>G, (d) MoO<sub>2</sub><sup>VI</sup>T and (e) MoO<sub>2</sub><sup>VI</sup>G.

water, while the second weight loss occurred in the range from 180–210 °C is ascribed to the decomposition of oxygen carrying functionalities [14,41,42]. However, the TG curve for the supported catalysts shows three step weight losses at temperatures ranged from 30 °C to 600 °C under N<sub>2</sub> atmosphere. Weight loss below 180 °C corresponds to the physically adsorbed water. Weight loss in the range of 180 to 250 °C is probably attributed to the decomposition of undigested oxygen carrying functionalities. Weight loss in the temperature range from 250 °C to 600 °C is allocated to the decomposition of the ligand. Weight losses of ca. 13.5% and 14.4% for the VO<sup>IV</sup>T and VO<sup>IV</sup>G were observed, respectively. The loadings of 8-quinolinol are 0.86 and 0.92 mmol/g calculated based on nitrogen analysis, which is consistent with the results of TG. Meanwhile the corresponding metal contents are 0.42 and 0.56 mmol/g estimated by ICP-AES, respectively. Consequently, the molar ratio of ligand/metal is 2.05 and 1.64 for the VO<sup>IV</sup>T and VO<sup>IV</sup>G, respectively, which is consistent with the increased heterogeneity of the active sites with a distribution of bis-1 and mono-1 ligated metals. Fig. 8 exhibits EPR spectra of the templated VO<sup>IV</sup>T and randomly grafted VO<sup>IV</sup>G materials. Obviously, compared with VO<sup>IV</sup>T, a slight signal broadening is observed in VO<sup>IV</sup>G, indicating that oxovanadium(IV)

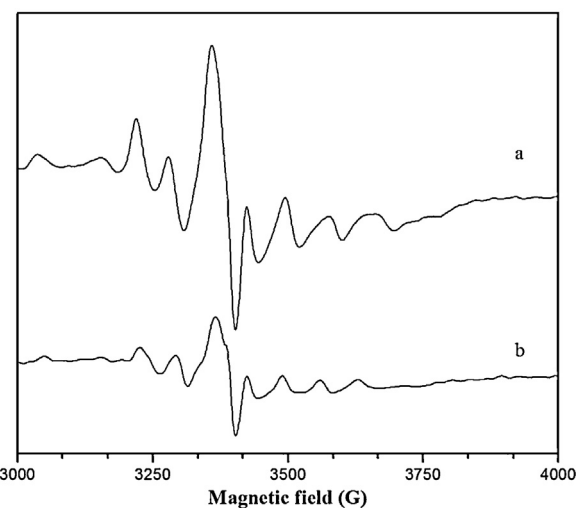


Fig. 8. Room temperature EPR spectra of VO<sup>IV</sup>T and VO<sup>IV</sup>G.

complex in the templated material has better site-isolation. Similar results were obtained for the MoO<sub>2</sub><sup>VI</sup>T and MoO<sub>2</sub><sup>VI</sup>G catalysts.

### 3.4. X-ray photoelectron spectroscopy studies

To investigate the surface constitution of the catalysts, the C1s, N1s and M2p (M=V or Mo) binding energies are studied, and the corresponding XPS spectrum of all the samples are presented in Fig. 9. The C1s spectrum of GO (Fig. 9a) suggests four types of sp<sup>2</sup>-hybridized C1s with four peaks centered at ca. 284.3, 285.4, 287.4, and 289.1 eV due to C=C, C-OH, C-O-C, and O-C=O groups, respectively, indicating that GO has been successfully synthesized [39]. Meanwhile, the C1s XPS spectrum of the other supported catalysts (Fig. 9b–e) also exhibits these same oxygen functionalities, and the intensity of C-OH signal decreased for these catalysts compared with the starting GO, suggesting that 8-quinolinol ligand is successfully immobilized onto GO. The binding energy of V2p for the VO<sup>IV</sup>T and VO<sup>IV</sup>G catalysts (Fig. 9 V2p) is 517.1 eV and 524.2 eV, respectively, which can be assigned to vanadium(IV) atom in the supported vanadium catalysts. The two peaks appeared at ca. 232.9 eV and 236.1 eV in the 3d orbitals are, respectively, due to Mo 3d<sub>5/2</sub> and Mo 3d<sub>3/2</sub> in the MoO<sub>2</sub><sup>VI</sup>T and MoO<sub>2</sub><sup>VI</sup>G catalysts (Fig. 9 Mo3d), indicating that the molybdenum species with such a binding energy could be assigned to Mo(VI). Correspondingly, the only peak appeared at ca. 399.1 eV in the 1s orbit is due to N1s for the MoO<sub>2</sub><sup>VI</sup>T and MoO<sub>2</sub><sup>VI</sup>G catalysts (Fig. 9 N1s), indicating that 8-quinolinol complexes have been prepared. Similar results were obtained for the vanadium catalysts (Fig. 2S N1s). It is consistent with the above mentioned conclusion.

### 3.5. Catalytic tests

The activity of the derivatized GO materials and the complexes (VO<sup>IV</sup>T, VO<sup>IV</sup>G and so on) as catalysts for the epoxidation of olefins was investigated using cyclooctene, styrene, 1-octene and geraniol as substrates and *t*-butylhydroperoxide (TBHP) as oxidant plus (CHCl<sub>3</sub> or CH<sub>3</sub>CN) as the solvent (Table 1). As expected, all catalysts are active for the epoxidation of olefins. By contrast, the catalytic results of the homogeneous complexes (VO<sup>IV</sup>N and MoO<sub>2</sub><sup>VI</sup>N), Zn<sup>II</sup>T, and randomly ligand-grafted heterogeneous analogue (VO<sup>IV</sup>G and MoO<sub>2</sub><sup>VI</sup>G) as catalysts are also given under the same conditions. When CH<sub>3</sub>CN was used as solvent and TBHP was used as oxidant, the VO<sup>IV</sup>T catalyst shows 79.4% conversion of cyclooctene with a TOF of 23.6 and 66.9% yield of the corresponding

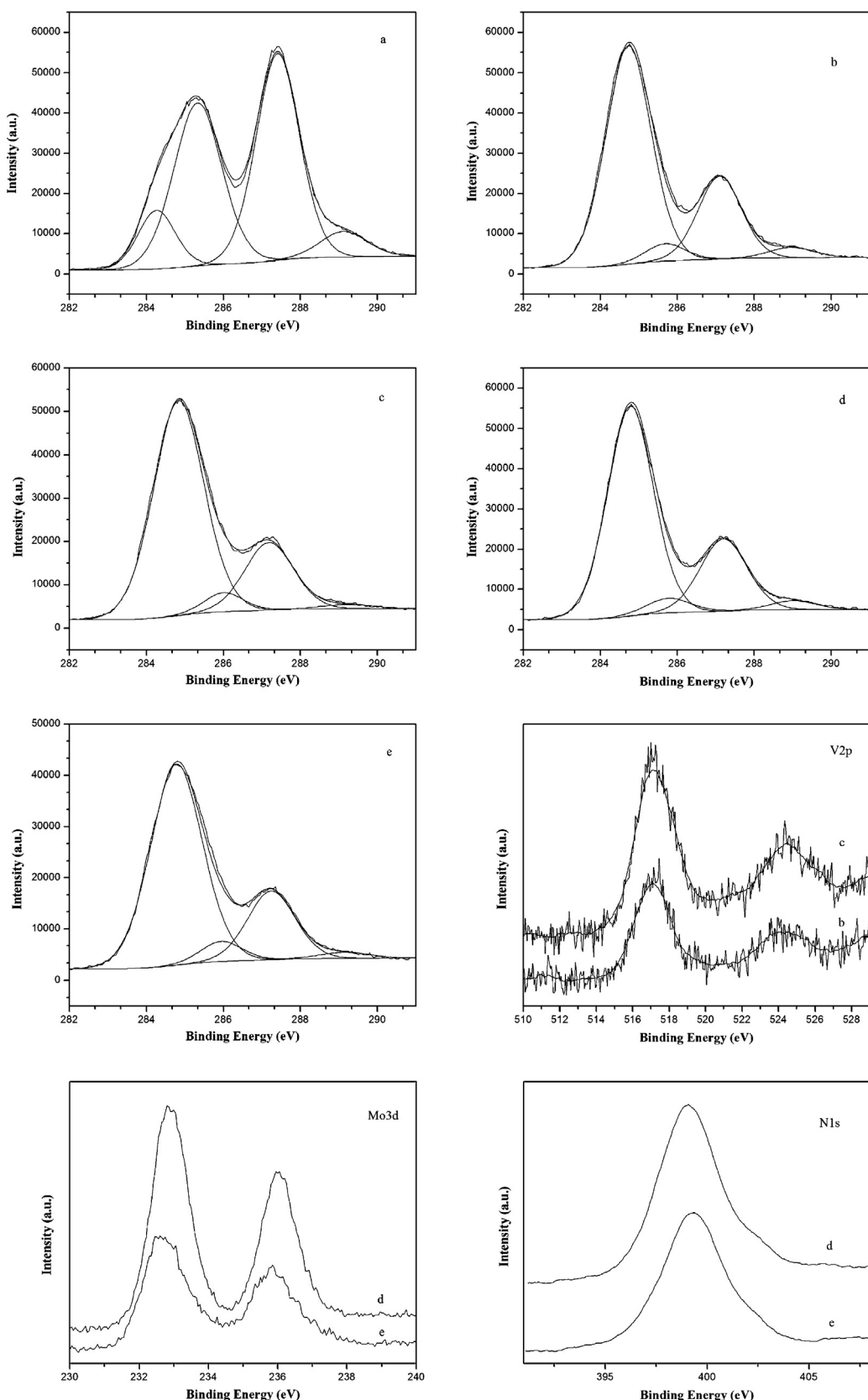


**Fig. 9.** XPS spectra of C (a) GO, (b)  $\text{VO}^{\text{IV}}\text{T}$ , (c)  $\text{VO}^{\text{IV}}\text{G}$ , (d)  $\text{MoO}_2^{\text{VI}}\text{T}$  and (e)  $\text{MoO}_2^{\text{VI}}\text{G}$ , V2p (b)  $\text{VO}^{\text{IV}}\text{T}$ , (c)  $\text{VO}^{\text{IV}}\text{G}$ , Mo3d and N1s (d)  $\text{MoO}_2^{\text{VI}}\text{T}$  and (e)  $\text{MoO}_2^{\text{VI}}\text{G}$ .

epoxide after 8 h. As for freshly prepared  $\text{MoO}_2^{\text{VI}}\text{T}$  catalyst, it shows high activity and good epoxide yield in  $\text{CHCl}_3$ , corresponding to 86.3% conversion of cyclooctene with a TOF of 30.8 and 86.3% yield of the corresponding epoxide. Nevertheless, homogeneous

complexes and randomly ligand-grafted heterogeneous catalysts show lower activity, turnover frequency and epoxide yields than the corresponding templated catalysts, suggesting that site-isolated bis-8-quinolinol coordination sphere prevents bimolecular

**Table 1**

Epoxidation catalyzed by various catalysts.

Catalysts	Oxidant	Solvent	Substrate	Metal content (mmol g <sup>-1</sup> )	Conversion <sup>a</sup> (%)	Epoxide yield (%)	TOF <sup>b</sup> (h <sup>-1</sup> )	Reference
Zn <sup>II</sup> T	TBHP	CH <sub>3</sub> CN	Cyclooctene	–	3.0	3.0	–	Herein
VO <sup>IV</sup> T	TBHP	CH <sub>3</sub> CN	Cyclooctene	0.420	79.4	66.9	23.6	Herein
VO <sup>IV</sup> T	H <sub>2</sub> O <sub>2</sub>	CH <sub>3</sub> CN	Cyclooctene	0.420	42.6	42.2	12.7	Herein
VO <sup>IV</sup> T	TBHP	CHCl <sub>3</sub>	Cyclooctene	0.420	40.8	40.4	12.1	Herein
VO <sup>IV</sup> T	TBHP	CH <sub>3</sub> CN	Geraniol	0.420	83.7	79.8	24.9	Herein
VO <sup>IV</sup> T	H <sub>2</sub> O <sub>2</sub>	CH <sub>3</sub> CN	Geraniol	0.420	96.2	43.4	28.6	Herein
VO <sup>IV</sup> T	TBHP	CH <sub>3</sub> CN	Styrene	0.420	50.6	2.3	15.1	Herein
VO <sup>IV</sup> T	TBHP	CH <sub>3</sub> CN	1-Octene	0.420	–	–	–	Herein
VO <sup>IV</sup> G	TBHP	CH <sub>3</sub> CN	Cyclooctene	0.560	64.0	52.5	14.3	Herein
VO <sup>IV</sup> G	H <sub>2</sub> O <sub>2</sub>	CH <sub>3</sub> CN	Cyclooctene	0.560	28.1	28.1	6.3	Herein
VO <sup>IV</sup> G	TBHP	CH <sub>3</sub> CN	Geraniol	0.560	80.0	76.3	17.9	Herein
VO <sup>IV</sup> G	H <sub>2</sub> O <sub>2</sub>	CH <sub>3</sub> CN	Geraniol	0.560	93.7	50.6	20.9	Herein
VO <sup>IV</sup> G	TBHP	CH <sub>3</sub> CN	Styrene	0.560	22.9	0.6	5.1	Herein
VO <sup>IV</sup> G	TBHP	CH <sub>3</sub> CN	1-Octene	0.560	–	–	–	Herein
VO <sup>IV</sup> N	TBHP	CH <sub>3</sub> CN	Cyclooctene	–	79.0	68.8	35.1	[29]
MoO <sub>2</sub> <sup>VI</sup> T	TBHP	CH <sub>3</sub> CN	Cyclooctene	0.350	28.2	27.6	10.1	Herein
MoO <sub>2</sub> <sup>VI</sup> T	TBHP	CHCl <sub>3</sub>	Cyclooctene	0.350	86.3	86.3	30.8	Herein
MoO <sub>2</sub> <sup>VI</sup> T	H <sub>2</sub> O <sub>2</sub>	CHCl <sub>3</sub>	Cyclooctene	0.350	26.0	25.7	9.3	Herein
MoO <sub>2</sub> <sup>VI</sup> T	TBHP	CHCl <sub>3</sub>	Geraniol	0.350	92.5	82.9	33.0	Herein
MoO <sub>2</sub> <sup>VI</sup> T	H <sub>2</sub> O <sub>2</sub>	CHCl <sub>3</sub>	Geraniol	0.350	93.3	93.2	33.3	Herein
MoO <sub>2</sub> <sup>VI</sup> T	TBHP	CHCl <sub>3</sub>	Styrene	0.350	19.5	4.5	7.0	Herein
MoO <sub>2</sub> <sup>VI</sup> G	TBHP	CHCl <sub>3</sub>	Cyclooctene	0.570	67.1	65.6	14.7	Herein
MoO <sub>2</sub> <sup>VI</sup> G	TBHP	CHCl <sub>3</sub>	Geraniol	0.570	82.9	77.9	18.2	Herein
MoO <sub>2</sub> <sup>VI</sup> G	H <sub>2</sub> O <sub>2</sub>	CHCl <sub>3</sub>	Geraniol	0.570	81.2	81.1	17.8	Herein
MoO <sub>2</sub> <sup>VI</sup> G	TBHP	CHCl <sub>3</sub>	Styrene	0.570	13.5	0.6	3.0	Herein
MoO <sub>2</sub> <sup>VI</sup> N	TBHP	CHCl <sub>3</sub>	Cyclooctene	0.240	75.2	75.2	39.1	Herein

<sup>a</sup> Reaction conditions: catalyst 10 mg, substrate 1 mmol, solvent 1 ml, oxidant 1 mmol, duration 8 h, and temperature 70 °C.<sup>b</sup> TOF, h<sup>-1</sup>: (turnover frequency) moles of substrate converted per mole metal ion per hour.

catalyst deactivation. The Zn<sup>II</sup>T catalyst shows only 3.0% conversion of cyclooctene under the same condition, which is almost parallel to the blank experiment (not show), indicating that the residual Zn template cannot play a catalytic role.

Furthermore, the influence of the solvents on the catalytic properties of various catalysts was also investigated. Table 1 summarizes catalytic results of these control experiments for the oxidation of cyclooctene. The VO<sup>IV</sup>T catalyst shows 79.4% conversion of cyclooctene after 8 h when using TBHP as the solvent in CH<sub>3</sub>CN, while it only shows 40.8% conversion of cyclooctene after 8 h when using TBHP as the solvent in CHCl<sub>3</sub>. However, the catalytic result of MoO<sub>2</sub><sup>VI</sup>T catalyst is almost opposite to that of VO<sup>IV</sup>T catalyst in CH<sub>3</sub>CN and CHCl<sub>3</sub>. It seems clear from this finding that the oxovanadium(IV) catalyst performs well with TBHP as the oxidant in CH<sub>3</sub>CN, while the molybdenum catalyst shows best performance with TBHP as the oxidant in CHCl<sub>3</sub>. This result is consistent with our early work [24,29].

Moreover, the results of the epoxidation of cyclooctene and geraniol using different oxidants over various catalysts (VO<sup>IV</sup>T, VO<sup>IV</sup>G, MoO<sub>2</sub><sup>VI</sup>T and MoO<sub>2</sub><sup>VI</sup>G) are also investigated (Table 1). It is obvious that the new heterogeneous catalysts showed comparable or even higher conversion in oxidation of geraniol using H<sub>2</sub>O<sub>2</sub> as oxidant under the similar reaction conditions as compared with the catalytic results using TBHP as oxidant. However, the catalytic results for the oxidation of cyclooctene are adverse, which might be attributed to the decomposing of H<sub>2</sub>O<sub>2</sub> into molecular oxygen and water [43,44]. The results demonstrate that H<sub>2</sub>O<sub>2</sub> is an appropriate oxidant in the oxidation of geraniol, while TBHP is an appropriate oxidant in the oxidation of cyclooctene.

In addition, the epoxidation of various substrates has been examined using the described reaction conditions (Table 1). The conversion of geraniol is the highest, followed by cyclooctene, while the conversion of 1-octene is the worst (no detectable conversion of 1-octene could be observed). It is probably due to electron density effect and hindrance effect [45].

The recoverability and stability of tethered the oxovanadium(IV) and molybdenum(VI) catalysts are also investigated by selecting the epoxidation of cyclooctene as a model reaction under similar

reaction conditions and the results are listed in Table 2. From what has been listed in Table 2, we can draw a conclusion that the VO<sup>IV</sup>T catalyst was far more stable than the VO<sup>IV</sup>G catalyst and could be successfully recycled for three times without evident loss of activity and selectivity in the same manner as that of the fresh catalysts, implying that the imprinted complex catalyst has improved stability and recycling due to better site-isolation. The catalytic activity of the VO<sup>IV</sup>G catalyst will decline sharply for three times. The recoverability results of MoO<sub>2</sub><sup>VI</sup>G catalyst was just the opposite, which may be due to some uncleared products on its surface.

The heterogeneous nature of catalysis over immobilized complexes has been tested in both of the catalytic reactions by leaching test. Leaching tests were performed for the catalysts VO<sup>IV</sup>T and MoO<sub>2</sub><sup>VI</sup>T which were filtered at the reaction temperature (80 °C). Half of the volume was filtered after reacting for 2 h and the resulting clear solution was permitted to react for another 6 h. The leaching results were listed in Fig. 10. This finding shows that cyclooctene could just be converted at a very low rate after filtrating VO<sup>IV</sup>T and MoO<sub>2</sub><sup>VI</sup>T catalysts. The filtrates were confirmed by ICP-AES. The results of the ICP analysis shows that the contents of vanadium and molybdenum for VO<sup>IV</sup>T and MoO<sub>2</sub><sup>VI</sup>T are 0.402 and 0.341 mmol/g, respectively, suggesting that the metal contents in the recovered catalyst were close to the fresh catalysts. Therefore, the large majority of the catalysis is carried out by truly heterogeneous oxovanadium(IV) and molybdenum(VI) catalysts.

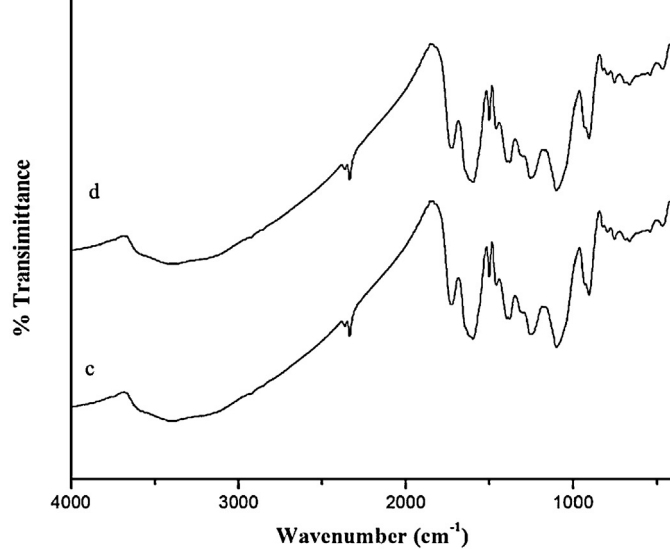
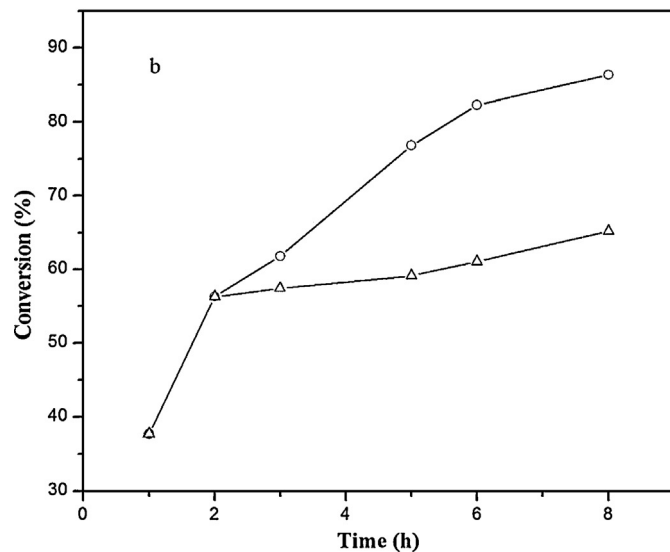
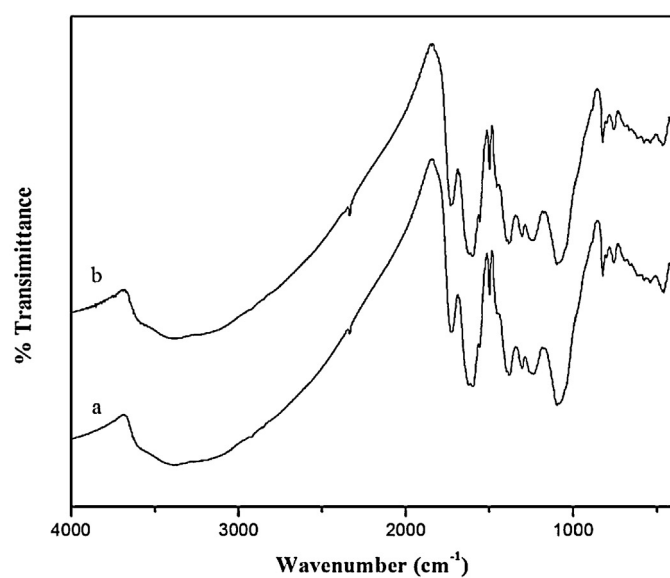
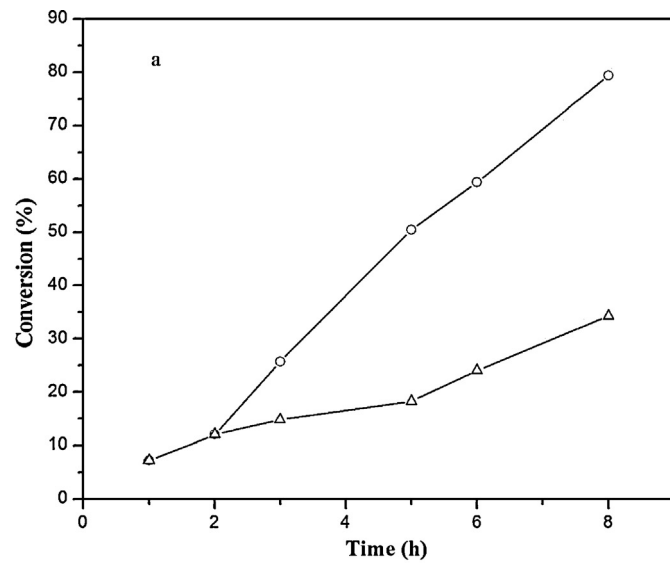
In order to characterize the recovered catalysts VO<sup>IV</sup>T and MoO<sub>2</sub><sup>VI</sup>T (after three cycles), FT-IR spectra (Fig. 11) were done for the recycled catalysts after three catalytic runs. IR spectra of recovered catalysts are found to be nearly identical to those of fresh catalysts, which indicate the stability and recoverability of the catalysts. These observations are in accordance with the result of the leaching test.

On the basis of our catalytic experimental data and comparison with the proposed mechanism reported in the literature of related systems [45,46], the probable reaction mechanism for the epoxidation of cyclooctene with TBHP over MoO<sub>2</sub><sup>VI</sup>T catalyst is proposed in Scheme 2: (1) the molybdenum(VI) complex (MoO<sub>2</sub><sup>VI</sup>L-GO 1) was coordinated to TBHP to produce a superoxo

**Table 2**

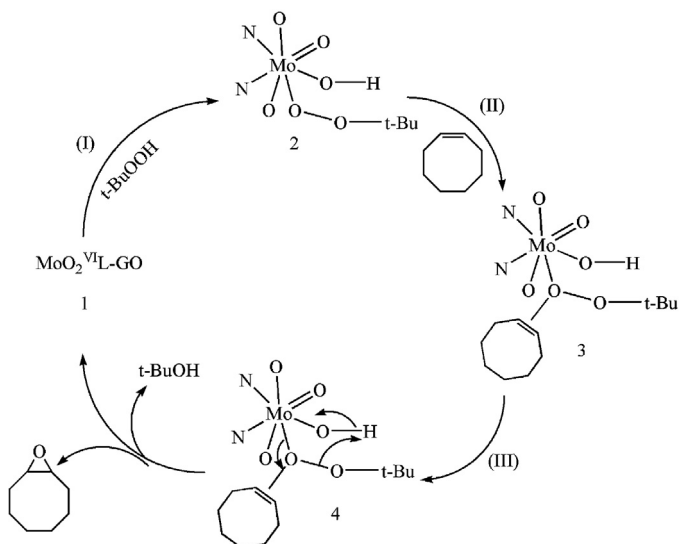
Epoxidation of cyclooctene by various catalysts.

Catalysts	Cycle	Solvent	Metal content (mmol g <sup>-1</sup> )	Conversion <sup>a</sup> (%)	Epoxide yield (%)	TOF <sup>b</sup> (h <sup>-1</sup> )
VO <sup>IV</sup> T	1	CH <sub>3</sub> CN	0.420	79.4	66.9	23.6
VO <sup>IV</sup> T	2	CH <sub>3</sub> CN	–	75.3	59.6	–
VO <sup>IV</sup> T	3	CH <sub>3</sub> CN	0.390	73.4	59.4	23.5
VO <sup>IV</sup> G	1	CH <sub>3</sub> CN	0.560	64.0	52.5	14.3
VO <sup>IV</sup> G	2	CH <sub>3</sub> CN	–	55.2	39.8	–
VO <sup>IV</sup> G	3	CH <sub>3</sub> CN	–	25.4	17.8	–
MoO <sub>2</sub> <sup>VI</sup> T	1	CHCl <sub>3</sub>	0.350	86.3	86.3	30.8
MoO <sub>2</sub> <sup>VI</sup> T	2	CHCl <sub>3</sub>	–	82.2	82.2	–
MoO <sub>2</sub> <sup>VI</sup> T	3	CHCl <sub>3</sub>	0.338	81.9	81.9	30.3
MoO <sub>2</sub> <sup>VI</sup> G	1	CHCl <sub>3</sub>	0.570	67.1	65.6	14.7
MoO <sub>2</sub> <sup>VI</sup> G	2	CHCl <sub>3</sub>	–	76.2	76.1	–
MoO <sub>2</sub> <sup>VI</sup> G	3	CHCl <sub>3</sub>	0.530	72.9	72.8	17.2

<sup>a</sup> Reaction conditions: catalyst 10 mg, cyclooctene 1 mmol, solvent 1 ml, TBHP 1 mmol, duration 8 h, and temperature 70 °C.<sup>b</sup> TOF, h<sup>-1</sup>: (turnover frequency) moles of substrate converted per mole metal ion per hour.

**Fig. 10.** Kinetic profile of aerobic epoxidation of cyclooctene (○) and leaching experiments of (a) VO<sup>IV</sup>T and (b) MoO<sub>2</sub><sup>VI</sup>T catalysts (△) (continuing the reaction after removing the catalyst after 2 h). Reaction conditions are analogous to Table 1. (a) VO<sup>IV</sup>T: oxidant (TBHP), solvent (CH<sub>3</sub>CN); (b) MoO<sub>2</sub><sup>VI</sup>T: oxidant (TBHP), solvent (CHCl<sub>3</sub>).

**Fig. 11.** FT-IR spectra of (a) the fresh catalyst VO<sup>IV</sup>T, (b) the used catalyst VO<sup>IV</sup>T for three cycles, (c) the fresh catalyst MoO<sub>2</sub><sup>VI</sup>T and (d) the used catalyst MoO<sub>2</sub><sup>VI</sup>T for three cycles.



**Scheme 2.** Reaction scheme involving two types of organometallic intermediates for cyclooctene epoxidation in presence of TBHP (*t*-BuOOH).

bonded intermediate 2. (2) The redox reaction of olefin substrate (cyclooctene) with a superoxo bonded intermediate 2 proceeded to form the cyclooctenic olefin intermediate 3. (3) The final products (cyclooctene oxide) formation can also be caused by migratory insertion and the molybdenum(VI) catalyst ( $\text{MoO}_2^{\text{VI}}\text{L-GO}$  1) was reproduced. Consequently, electron-rich olefins react faster than electron-poor olefins due to reaction of an olefin as a nucleophile with oxygen as an electrophile.

#### 4. Conclusions

A synthetic metal-template/metal-exchange method to imprint the covalent attachment of discrete bis(8-quinolinol) oxovanadium(IV) or bis(8-quinolinol)dioxomolybdenum(VI) complex onto monolayer graphene oxide (GO) is reported herein together with their catalytic activities for the epoxidation of alkenes. The prepared catalysts were characterized by XRD, N<sub>2</sub> adsorption/desorption, TEM, FT-IR, diffusion reflection UV-visible, ICP-AES, TG, Raman, EPR, N element analysis and XPS, suggesting that oxovanadium(IV) or dioxomolybdenum(VI) catalysts have been successfully prepared. The templated oxovanadium(IV) or dioxomolybdenum(VI) catalysts exhibit better selectivity and more efficient catalytic activity for olefin epoxidation with TBHP or H<sub>2</sub>O<sub>2</sub> than the analogous homogeneous catalyst or grafted catalyst under the same conditions. Moreover, these imprinted complexes catalysts have improved stability and recycling due to better site-isolation. Future reports will describe the immobilization of other transition metals catalysts that require bidentate or multiple ligands in the epoxidation of alkenes by the metal-template/metal-exchange method.

#### Acknowledgments

This work was supported by the National Natural Science Foundation of China (21303069), Jilin province (201105006), and Jilin University (450060445017).

#### Appendix A. Supplementary data

Supplementary data associated with this article can be found, in the online version, at <http://dx.doi.org/10.1016/j.apcata.2013.10.037>.

#### References

- [1] B. Notari, Studies in Surface Science Catalysis 60 (1991) 343–351.
- [2] G. Barf, R. Sheldon, Journal of Molecular Catalysis A: Chemical 102 (1995) 23–39.
- [3] J.R. Monnier, Applied Catalysis A: General 221 (2001) 73–91.
- [4] L. Wang, H. Wang, P. Hapala, L. Zhu, L. Ren, X. Meng, J.P. Lewis, F.S. Xiao, Journal of Catalysis 281 (2011) 30–39.
- [5] X.T. Zhou, Q.H. Tang, H.B. Ji, Tetrahedron Letters 50 (2009) 6601–6605.
- [6] G. Grivani, G. Bruno, H.A. Rudbari, A.D. Khalaji, P. Pourteimouri, Inorganic Chemistry Communications 18 (2012) 15–20.
- [7] M.G. Topuzova, S.V. Kotov, T.M. Kolev, Applied Catalysis A: General 281 (2005) 157–166.
- [8] H. Kameyama, F. Narumi, T. Hattori, H. Kameyama, Journal of Molecular Catalysis A: Chemical 258 (2006) 172–177.
- [9] B. Gong, X. Fu, J. Chen, Y. Li, X. Zou, X. Tu, P. Ding, L. Ma, Journal of Catalysis 262 (2009) 9–17.
- [10] D.E. De Vos, B.F. Sels, P.A. Jacobs, Advances in Catalysis 46 (2001) 1–87.
- [11] D.E. De Vos, B.F. Sels, P.A. Jacobs, Advanced Synthesis and Catalysis 345 (2003) 457–473.
- [12] T.J. Terry, T.D.P. Stack, Journal of the American Chemical Society. 130 (2008) 4945–4953.
- [13] T.J. Terry, G. Dubois, A. Murphy, T.D.P. Stack, Angewandte Chemie 119 (2007) 963–965.
- [14] H.P. Mungse, S. Verma, N. Kumar, B. Sain, O.P. Khatri, Journal of Materials Chemistry 22 (2012) 5427–5433.
- [15] D.A. Dikin, S. Stankovich, E.J. Zimney, R.D. Piner, G.H. Dommett, G. Evmenenko, S.T. Nguyen, R.S. Ruoff, Nature 448 (2007) 457–460.
- [16] D.R. Dreyer, S. Park, C.W. Bielawski, R.S. Ruoff, Chemical Society Reviews 39 (2010) 228–240.
- [17] O.C. Compton, S.T. Nguyen, Small 6 (2010) 711–723.
- [18] G. Wang, X. Sun, C. Liu, J. Lian, Applied Physics Letters 99 (2011), 053114-053114-3.
- [19] K. Krishnamoorthy, R. Mohan, S.J. Kim, Applied Physics Letters 98 (2011) 244101–244103.
- [20] U. Khan, P. May, A. O'Neill, J.N. Coleman, Carbon 48 (2010) 4035–4041.
- [21] Q. Cheng, J. Tang, J. Ma, H. Zhang, N. Shinya, L.C. Qin, Carbon 49 (2011) 2917–2925.
- [22] W.S. Hummers Jr., R.E. Offeman, Journal of the American Chemical Society 80 (1958) 1339.
- [23] A.V. Talyzin, B. Sundqvist, T. Szabo, I. Dekany, V. Dmitriev, Journal of the American Chemical Society 131 (2009) 18445–18449.
- [24] Y. Yang, S. Hao, Y. Zhang, Q. Kan, Solid State Sciences 13 (2011) 1938–1942.
- [25] Y. Yang, Y. Zhang, S. Hao, J. Guan, H. Ding, F. Shang, P. Qiu, Q. Kan, Applied Catalysis A: General 381 (2010) 274–281.
- [26] Y. Lin, J. Jin, M. Song, Journal of Materials Chemistry 21 (2011) 3455–3461.
- [27] P. Liu, K. Gong, P. Xiao, M. Xiao, Journal of Materials Chemistry 10 (2000) 933–935.
- [28] K. Krishnamoorthy, M. Veerapandian, K. Yun, S.J. Kim, Carbon 53 (2012) 38–49.
- [29] Y. Yang, Y. Zhang, S. Hao, Q. Kan, Catalysis Communications 11 (2010) 808–811.
- [30] Y. Yang, Y. Zhang, S. Hao, Q. Kan, Journal of Colloid and Interface Science 362 (2011) 157–163.
- [31] Y. Zu, J. Tang, W. Zhu, M. Zhang, G. Liu, Y. Liu, W. Zhang, M. Jia, Bioresource Technology 102 (2011) 8939–8944.
- [32] D. Pan, S. Wang, B. Zhao, M. Wu, H. Zhang, Y. Wang, Z. Jiao, Chemistry of Materials 21 (2009) 3136–3142.
- [33] D. Long, W. Li, L. Ling, J. Miyawaki, I. Mochida, S.H. Yoon, Langmuir 26 (2010) 16096–16102.
- [34] F. Liu, J. Sun, L. Zhu, X. Meng, C. Qi, F.S. Xiao, Journal of Materials Chemistry 22 (2012) 5495–5502.
- [35] M. Salavati-Niasari, M. Bazarganipour, Catalysis Communications 7 (2006) 336–343.
- [36] F. Tuinstra, J.L. Koenig, The Journal of Chemical Physics 53 (1970) 1126–1130.
- [37] J. Wu, D. Zhang, Y. Wang, Y. Wan, B. Hou, Journal of Power Sources 198 (2012) 122–126.
- [38] S. Choudhary, H.P. Mungse, O.P. Khatri, Journal of Materials Chemistry 22 (2012) 21032–21039.
- [39] Z.G. Le, Z. Liu, Y. Qian, C. Wang, Applied Surface Science 258 (2012) 5348–5353.
- [40] W. Ai, J.Q. Liu, Z.Z. Du, X.X. Liu, J.Z. Shang, M.D. Yi, L.H. Xie, J.J. Zhang, H.F. Lin, T. Yu, RSC Advances 3 (2013) 45–49.
- [41] S. Stankovich, D.A. Dikin, R.D. Piner, K.A. Kohlhaas, A. Kleinhammes, Y. Jia, Y. Wu, S.T. Nguyen, R.S. Ruoff, Carbon 45 (2007) 1558–1565.
- [42] A. Lerf, H. He, M. Forster, J. Klinowski, The Journal of Physical Chemistry B 102 (1998) 4477–4482.
- [43] J. Tang, Y. Zu, W. Huo, L. Wang, J. Wang, M. Jia, W. Zhang, W.R. Thiel, Journal of Molecular Catalysis A: Chemical 355 (2012) 201–209.
- [44] S. McCann, M. McCann, M.T. Casey, M. Jackman, M. Devereux, V. McKee, Inorganica Chimica Acta 279 (1998) 24–29.
- [45] M. Masteri-Farahani, F. Farzaneh, M. Ghani, Catalysis Communications 8 (2007) 6–10.
- [46] Y. Li, X. Fu, B. Gong, X. Zou, X. Tu, J. Chen, Journal of Molecular Catalysis A: Chemical 322 (2010) 55–62.